https://doi.org/10.17221/191/2022-JFS

Sap flow modelling based on global radiation and canopy parameters derived from a digital surface model

Tomáš Mikita, Zdeněk Patočka, Elizaveta Avoiani*

Department of Forest Management and Applied Geoinformatics, Faculty of Forestry and Wood Technology, Mendel University in Brno, Brno, Czech Republic

**Corresponding author: zdenek.patocka@mendelu.cz*

Citation: Mikita T., Patočka Z., Avoiani E. (2023): Sap flow modelling based on global radiation and canopy parameters derived from a digital surface model. J. For. Sci., 69: 348–359.

Abstract: Sap flow represents water transport from roots to leaves through the xylem and is used to describe tree transpiration. This paper proposed and tested a procedure to estimate sap flow by calculating global radiation in a digital model of the tree canopy surface obtained by unmanned aerial vehicle imaging. The sap flow of nine trees was continuously measured in the field. In the digital surface model, individual canopies were automatically delineated, their parameters were determined and the global radiation incident on their surface on specific days was calculated. A polynomial relationship was found between sap flow and the calculated incident solar radiation during the morning hours with a coefficient of determination of 0.98, as well as a linear relationship between the decrease in radiation and sap flow during the afternoon with a correlation coefficient of 0.99. Using the Random Forest machine learning method, a model predicting the sap flow of the trees was created based on the global radiation and canopy parameters determined from the digital surface model of tree canopies. The resulting model was deployed on additional days and compared to field measurements of sap flow, achieving a correlation coefficient of 0.918. In addition, two linear regression models were created for a tree group, achieving coefficients of determination of 0.66 and 0.90.

Keywords: GIS; Random Forest; remote sensing; solar radiation; transpiration; unmanned aircraft vehicle (UAV)

Whole tree estimates of water use are becoming increasingly important in forest science (Wullschleger et al. 1998). Forest hydrologists rely on such information to help resolve issues of water resource management (Schiller, Cohen 1995; Loustau et al. 1996), as well as to evaluate the role of transpiration in forest and woodland hydrology (Barrett et al. 1996; Kupec, Deutscher 2017). The effect of transpiration has also been linked to intra-daily variations in streamflows in forest stands, although, so far, there is no generally accepted model to explain how streamflow declines

Supported by the Ministry of Agriculture of the Czech Republic, grant No. QK1810415 'Influence of forest stands species composition and structure on microclimate and landscape hydrology'.

https://doi.org/10.17221/191/2022-JFS

due to transpiration occurrence (Bond et al. 2002; Gribovszki et al. 2008; Wondzell et al. 2009). Thus, empirical models are used to calculate transpiration at the forest stand level, e.g. based on regression analysis between stem diameter at breast height and the corresponding tree water consumption (Čermák et al. 2004), with subsequent modelling of transpiration using the Penman-Monteith model (Allen et al. 1998).

The main methods developed for sap flow measurements are heat pulse velocity (HPV; e.g. Huber 1932; Caspari 1993), trunk segment heat balance (THB; Čermák, Deml 1974; Kučera et al. 1977); stemheat balance (SHB; Sakuratani 1981; Baker, van Bavel 1987), heat dissipation (HD; Granier 1985) or heat field deformation (HFD; Nadezhdina et al. 1998). In the Czech Republic, the trunk heat balance method is the most used and developed. The original THB method, characterised by direct electric heating and internal sensing of temperature, was originally designed for large trees (Čermák, Deml 1974; Čermák et al. 2004). A section of a large tree trunk is heated from the inside by an electric current (supplied by electrodes) passing through the tissues.

Sap flow is controlled by environmental variables, such as vapour pressure deficit (VPD), solar radiation (Rad), air temperature, wind speed, soil water, and soil temperature. However, the impact of each variable on sap flow varied with climatic region, species composition, and age of the trees. Vapour pressure deficit and solar radiation are the main drivers of sap flow (Oogathoo et al. 2020). Solar radiation information over large territories can be provided by models that are taking into consideration the surface inclination, aspect, and shadowing effects. These models can be useful for predicting solar radiation in areas without measured data (Choi et al. 2019). Solar radiation models in GIS environments include the r.sun module in GRASS GIS software (Hofierka, Šúri 2002) or Area Solar Radiation in ArcGIS software (Rich et al. 1994; Fu 2000; Rich, Fu 2000). High-resolution surface data are needed to calculate solar radiation at the forest stand or individual tree level. These data can be obtained with either airborne or terrestrial methods, or by unmanned aircraft. Airborne laser scanning (ALS) has metric to decimetric resolution (Shan, Toth 2017), relatively rapid acquisition, the ability to detect multiple surface points from vegetation, and could be used even over a large area. Unmanned aircraft vehicles (UAVs) can be used to create highly detailed digital surface models (DSMs) with resolution down to the centimetre scale (Janata et al. 2016). Both methods allow relatively detailed modelling of the tree canopy (in the growing season). When calculating solar radiation, it is thus possible to calculate the radiation incoming on a particular tree during the day.

Some studies have considered that so-called effective solar radiation (ESR) has a direct (Xu, Ma 2007) or indirect (Martin 1999) effect on sap flow activity. Relationships between the time process of sap flow and ESR in these studies were limited to a few days. Studies dealing with evapotranspiration prediction from UAV data focus on different terrestrial ecosystems (Brenner et al. 2017, Niu et al. 2020). For the complex study of relationships between evapotranspiration and its controlling factors, it is common to use statistical regression models and machine learning (ML) algorithms such as Random Forest (RF) or artificial neural networks (ANN) (Feng et al. 2017; Dou, Yang 2018; Ellsäßer et al. 2020).

In this paper, our objectives were: (*i*) to find the methodology on how to access global solar radiation for individual tree crowns based on UAV data, (*ii*) to describe the daily and seasonal temporal variation of sap flow in relationship with global forest radiation calculated for whole crowns, (*iii*) to create some quantitative relationship between global solar radiation and sap flow and principal tree parameters, and (*iv*) to apply the established relationship to entire forest stands.

MATERIAL AND METHODS

The study was carried out in the Rájec-Němčice research area (Figure 1). The Rájec-Němčice research plot was established in 1968 by the Institute of Forest Ecology (Mendel University in Brno) in connection with the UNESCO International Biological Programme (IBP) and the UNESCO Man and the Biosphere (MaB) international programme. It is a 100-year-old spruce stand located at an altitude of 633 m a.s.l.

Sap flow measurement. Continuous sap flow measurements were performed on only 9 selected trees using the EMS81 sap flow system (Environmental Measuring Systems, Czech Republic), which is composed of sap flow module SF 8X (SDI-12)

https://doi.org/10.17221/191/2022-JFS

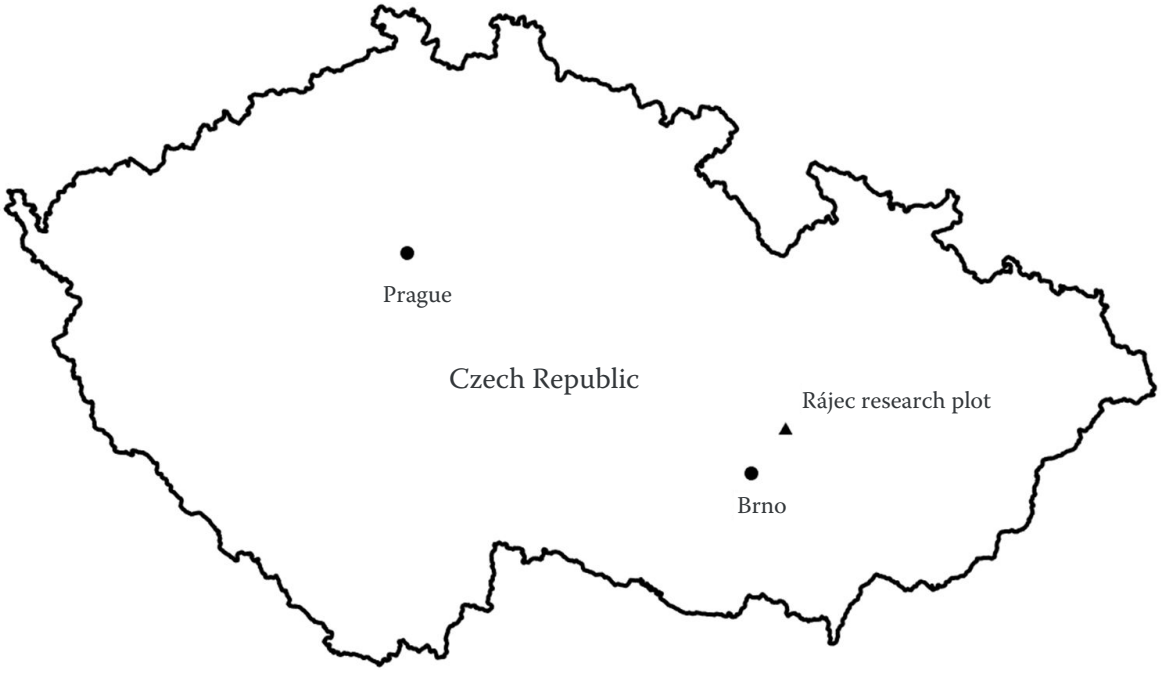

Figure1. Location of the research plot Rájec-Němčice

and sap flow sensor SF 81. The stainless electrodes (terminals) were hammered into the stem and thermosensor needles were inserted into the geometrical centre of the part of the electrode inside the xylem. Highly conductive steel equalises radial differences in temperature of the sapwood and allows measurement of mean xylem temperature. The measuring point at the tree is protected against ambient factors, mainly against direct sun irradiation, by using reflective insulating weather shields. The temperature of the heated xylem is measured by needle sensors inserted in slots to the geometrical centre of the electrodes' active part. Reference temperature related to the nonheated part of the stem is measured in the slot as well, in the same type of electrode installed 100 mm downwards. The heat balance of the xylem through which sap flows can be described by the general Equation (1):

$$P = Q \times dT \times c_w + dT \times z \quad (1)$$

where:

P – power of heat input (W);

Q – sap flow rate (kg·s^{-1});

dT – temperature difference within the measuring point;

c_w – specific heat of water (J·kg^{-1}·K^{-1});

z – coefficient of heat losses from the measuring point (W·K^{-1}).

The amount of water in terms of mass or volume passing through the measuring point in a stem is calculated from the power input and temperature rise of water passing through the heated space. Sap flow calculation is derived from the following Equation (2):

$$Q = \frac{P}{c_w \times d \times dT} - \frac{z}{c_w} \quad (2)$$

where:

d – effective width of the measuring point (5.5 cm).

The first term of this equation quantifies the amount of heat that is lead away by sap flow. The second term represents heat loss from the sensor. This loss can be estimated when sap flow approaches zero, i.e. during the rain or at night before sunrise (EMS 2018).

The tree positions were located geodetically using Trimble M3 total station (Trimble Inc., USA). Those coordinates served for the identification of each tree in the canopy height model to track changes at the tree level. Furthermore, continuous meteorological and climate data from a meteorological station located on a 35-meter-high tower were measured. Specifically, precipitation, air temperature and humidity data were used.

UAV data acquisition. The original intent of the study was to detect the change in canopy tem-

https://doi.org/10.17221/191/2022-JFS

perature during the day and find its dependence on sap flow. Therefore, several image data acquisitions of the study area were conducted in 2019 using a DJI Mavic 2 Enterprise drone (Shenzhen DJI Sciences and Technologies Ltd., China) with both RGB and thermal cameras at hourly intervals. However, the surface temperature of the tree canopy is influenced by a number of external factors (incoming solar radiation, humidity, wind strength, etc.) and no significant differences in the canopy temperature were found between multitemporal thermal data and no dependence between surface temperature and sap flow was detected. The accuracy of thermal imagery is dependent on several parameters (thermal camera settings and calibration, image resolution, area size, canopy illumination, etc.). The DJI Mavic 2 Enterprise is equipped with a non-radiometric thermal camera only. This means it can only detect differences in temperature. It is necessary to use a radiometric camera to accurately measure temperatures. It is then possible to specify the emissivity of the measured materials, humidity and air temperature at the time of flight. Therefore, the dependencies between the sap flow of individual trees and the total global radiation incoming on the tree canopy during the day were investigated. The entire research plot was imaged using a drone from a height of 80 m above the terrain with a longitudinal and lateral image overlap of 80%. Based on the photogrammetric processing of RGB images, a point cloud was created in Agisoft Metashape software (Version 1.6.0, 2019), followed by a detailed DSM and an orthophoto with a resolution of 10 cm. The created DSM was used for subsequent calculation of global radiation in ArcGIS Pro software (Version 3.0, 2022) using the Area Solar Radiation tool.

Solar radiation calculation. The Area Solar Radiation tool derives the incoming solar radiation from a raster DSM. The input file is the DSM of the area of interest and the output is a solar radiation model for the whole area with units of watt hours per square meter ($Wh \cdot m^{-2}$). The calculation is performed for each pixel of the input raster. Solar Radiation tool performs calculation for the entire landscape or specific locations based on methods from hemispheric visibility algorithms (Rich et al. 1994; Fu 2000; Rich, Fu 2000). The total radiation is calculated for specific areas or territories as global radiation. The calculations of direct, diffuse, and summed global radiation are repeated for each area on the topographic surface. The output is solar radiation maps for the whole area of input DSM. In the calculation of global radiation, direct and diffuse radiation is considered while reflected radiation is ignored. The atmospheric transmittance ratio and the diffuse component of the radiation can also be adjusted within the tool.

The calculation of global radiation consists of 4 basic steps: (*i*) calculation of the hemispheric sky visibility map in the zenith direction (Figure 2), (*ii*) overlaying the visibility map with a map of the Sun's motion to calculate the direct radiation, (*iii*) overlaying the visibility map with the sky map to calculate diffuse radiation, and (*iv*) repeating this process for each pixel of the input raster (Figure 3).

Tree crown detection. Due to previous geodetic surveying of trees fitted with sap flow sensors, it was possible to detect these trees on the DSM.

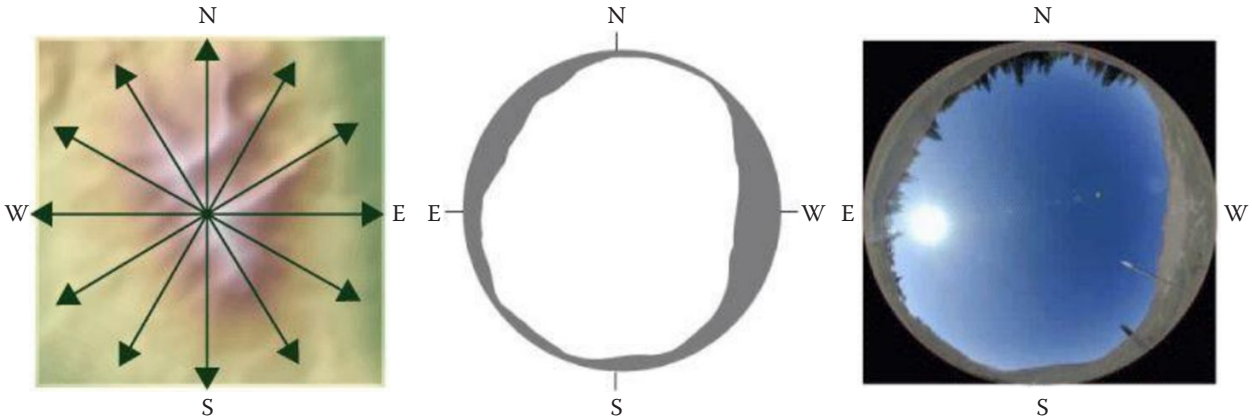

Figure 2. Calculation of the hemispheric visibility map (ESRI 2020)

https://doi.org/10.17221/191/2022-JFS

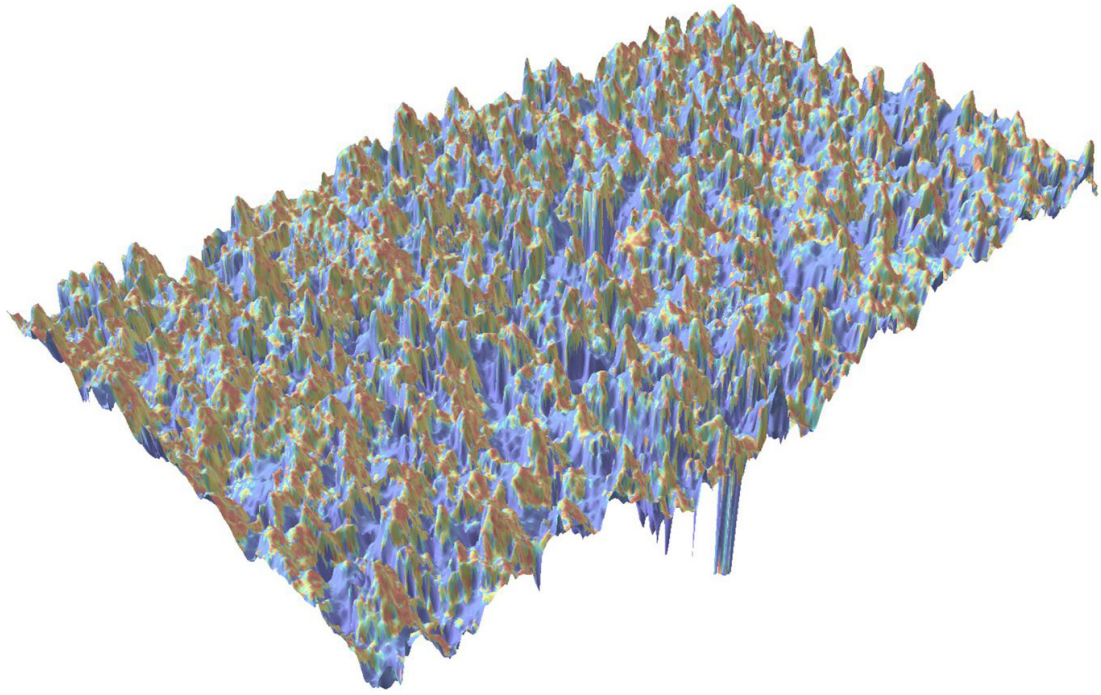

Figure 3. 3D visualisation of calculated global radiation for the locality Rájec from August 28, 2019

Based on the so-called inverse watershed analysis, the individual tree canopies were detected (Vincent, Soille 1991; Mikita et al. 2013) and their area, volume and canopy surface in 3D space were calculated (Figure 4).

Creation of a model for calculating sap flow from DSM. Sap flow data for individual trees were provided by Czechglobe (Global Change Research Institute CAS) for two days of the year 2019 (August 28 and September 12) and for the whole year 2020. The calculation of global radiation in GIS can be limited to any period and any interval even within one day.

Firstly, global radiation was calculated for the two specific days of the year 2019 at intervals of 10 minutes so that the values correspond to the sap flow

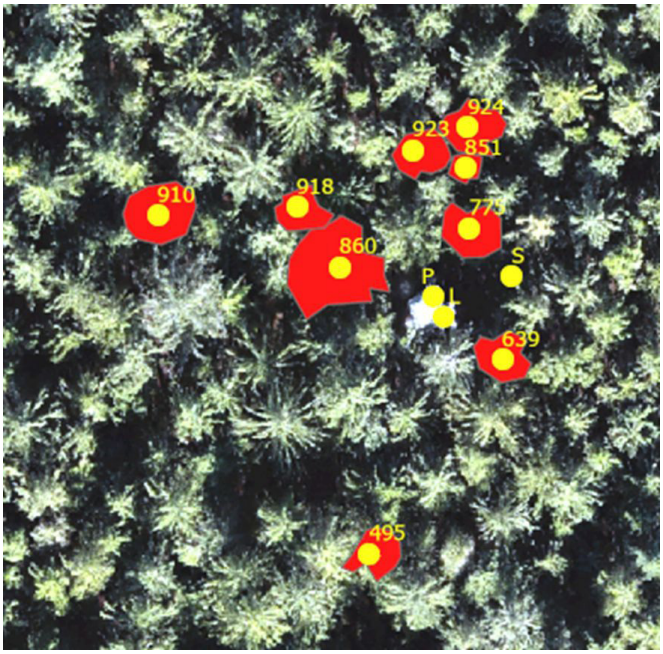

Figure 4. Detected tree crowns fitted with sap flow sensors

https://doi.org/10.17221/191/2022-JFS

measurement times. The global radiation values were related to the position of each tree canopy (trees with sap flow sensors) and the sum of radiation incoming on the canopy was calculated for each time interval.

Subsequently, the dependence of the daily sum of sap flow and total daily radiation was investigated for selected days throughout the growing season. Thus, a total of 13 days from the beginning to the end of the growing season (April 15 to October 15) were selected at a 14-day interval. For these days, based on the data provided by the weather station and sap flow sensor, the sum of sap flow, average daily temperature, average humidity and the sum of rainfall in the previous 14 days were calculated. The sum of global daily radiation was calculated once more for these days in ArcGIS Pro software. The dependence within selected days and the whole growing season was determined by linear regression.

RESULTS

Analysis of the correlation between sap flow and radiation shows a linear dependence of the increase of both values in the morning hours, and conversely a non-linear dependence of the decrease of values in the afternoon hours (Figure 5). At the same time, however, each tree responds differently to incoming light.

The increase and decrease of sap flow as a function of radiation has a similar pattern on August 28, 2019. If we average all values and trees for both days, we get a clear linear dependence of the increase and a non-linear dependence of the decrease of values (Figure 6).

The results show a very significant link between sap flow and DSM-based global radiation calculations. The calculation of radiation using GIS tools with accurate DSM allows to determine the amount of light incoming on the canopy of an individual tree during the day. However, this information does not allow for an area-based estimate of forest stand transpiration from DMP data. Therefore, other variables that may influence total daily transpiration were sought out. These variables can be numerous, e.g. cloud cover, humidity, soil water saturation after previous rainfall, etc. However, these variables are highly variable in time and space and thus only factors that are directly detectable from the Remote Sensing data (or UAV imagery) were chosen and supplemented by basic climatic factors.

The following variables were therefore chosen: (*i*) canopy area, (*ii*) canopy surface in 3D space, (*iii*) total sum of daily global radiation, (*iv*) canopy volume, (*v*) air humidity, (*vi*) mean daily temperature, and (*vii*) precipitation amount in previous 14 days.

A model predicting the sap flow of individual trees on specific days was created using the daily sum of global radiation incidents on the tree canopy and the canopy parameters with weather conditions at the day of measurement. The Random Forest machine learning method was used to create the model. First, all available predictors were used and then, five significant predictors that

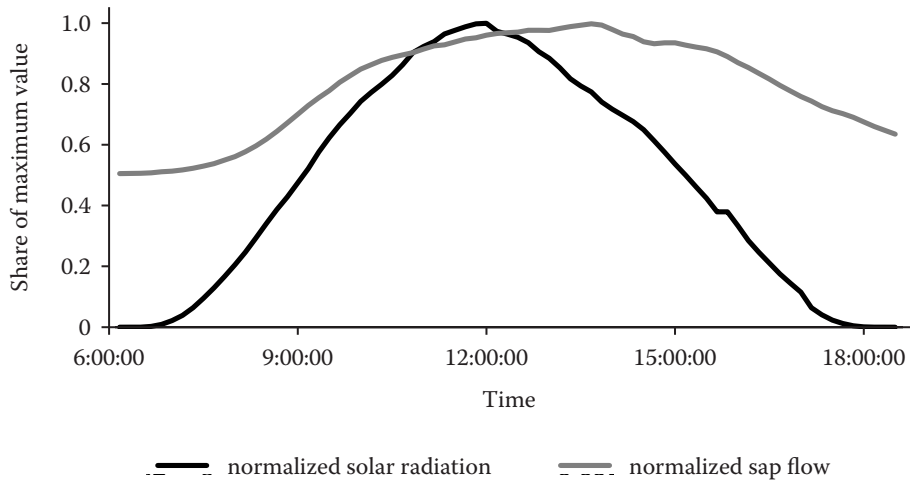

Figure 5. Normalized daily sap flow and calculated solar radiation on September 12, 2019

Mean values for all measured trees

https://doi.org/10.17221/191/2022-JFS

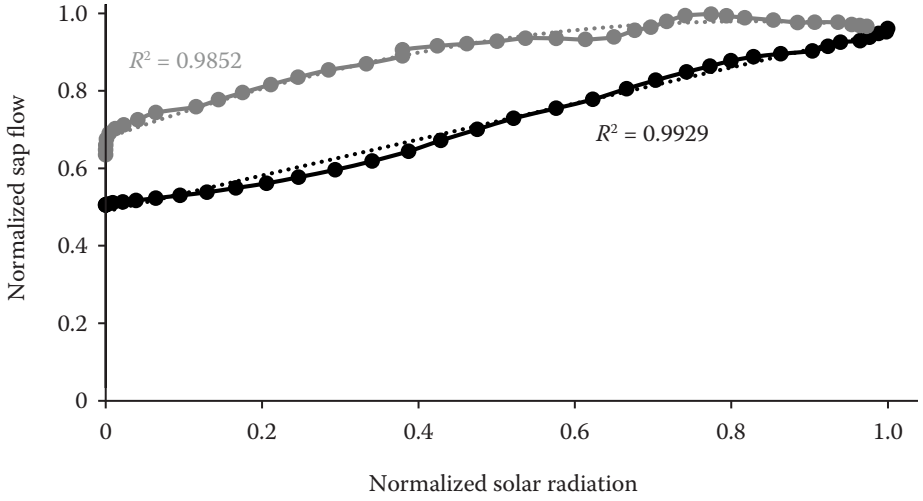

Figure 6. Increase and decrease of normalized sap flow as a function of normalized solar radiation on September 12, 2019
Mean values for all measured trees, grey line and dots – dawn to midday, black line and dots – from midday to evening

best reflected the variability of sap flow were selected based on the Predictor Importance parameter. The order of Predictor Importance (*PI*) was as follows: canopy volume (*PI* = 1.0000), air humidity (*PI* = 0.8766), total sum of daily global radiation (*PI* = 0.7748), canopy surface (*PI* = 0.7670) and canopy area (*PI* = 0.7670). The total daily sap flow of a specific tree for a particular day was entered into the model as the dependent variable (observed value); the predictors were the daily sum of global radiation incidents on the crown of a specific tree on a particular day, canopy volume, canopy surface, canopy area of a specific tree and the air humidity at the day of measurement. The model was trained in Tibco Statistica 13 software (Version 13.4.0.14, 2022). The data were randomly divided into training and test sets in a 70 : 30 ratio. Each model tree contained five predictors and a final collection of twenty trees was created. The error rates of the Random Forest model for each dataset and the overall error rate are shown in Table 1.

Furthermore, external validation of the model was performed for three additional days that were not included in the model training process (June 28, May 20, and August 8). The statistical evaluation of the success of the model deployment is presented in Table 1. The developed model was then applied to a part of the forest stand (Figure 7).

Since it has been shown that canopy parameters, in addition to radiation and air humidity, also affect sap flow, the sum of sap flow and radiation of all trees was summed. After that, a linear regression model of the dependence of sap flow of a group of trees on the total daily incoming radiation was created. The estimates of the regression parameters are in Table 2 and the statistical evaluation of the regression model is presented in Table 3. The model achieved a coefficient of determination of 0.66 and a normalized root mean square error *NRMSE* of 28.85%. The following regression triplet tests were performed: Fisher-Snedecor overall test, Scott's multicollinearity criterion, Cook-Weisberg test for heteroscedasticity, Jarque-Berra test for

Table 1. Statistical evaluation on train samples

Statistical measure	Train samples	Test samples	All samples	External validation
Mean square error	926.88	923.34	925.67	4 764.88
Mean absolute error	20.70	26.06	22.53	51.82
Mean relative squared error	0.08	0.1122	0.09	0.18
Mean relative absolute error	0.19	0.26	0.21	0.34
Correlation coefficient	0.97	0.96	0.97	0.92

https://doi.org/10.17221/191/2022-JFS

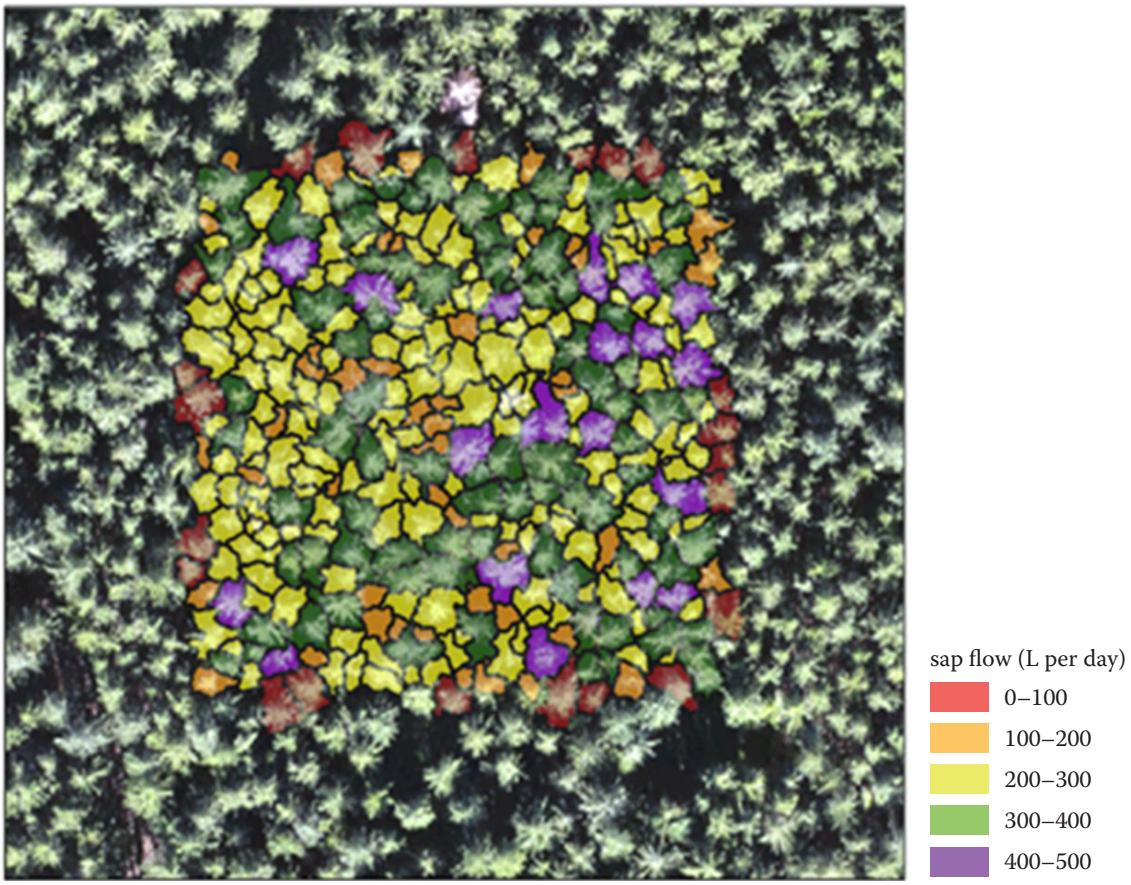

Figure 7. Calculation of the total daily sap flow based on the Random Forest model for a part of the forest stand within August 28, 2020

normality, Wald test for autocorrelation, Durbin-Watson test for autocorrelation, and sign test. No negative conclusions affecting the credibility of the model were found based on the regression triplet testing.

It was also possible to create a multiple regression model with independent variables of radiation and air humidity, which achieved a coefficient of determination of R^2 = 0.90 and *NRMSE* = 15.96% (Tables 4 and 5). Based on Scott's criterion, the multicollinearity of the model was found, and the sign test revealed a trend in the residuals. Multicollinearity was not confirmed by variance inflation factor (*VIF* = 1.84). Although this model has a higher regression rebate, there is a higher risk of overfitting compared to the first model.

Table 2. Parameter of regression model for sap flow estimation of tree group (model 1)

Variable	Estimate	Standard deviation	*P*-value	Lower limit	Upper limit
Radiation	2.56×10^{-5}	1.92×10^{-6}	1.54×10^{-8}	2.14×10^{-5}	2.98×10^{-5}

Table 3. Statistical evaluation of regression model for sap flow estimation of tree group (model 1)

Statistical measure	Value
Coefficient of determination (R^2)	0.66
Root mean square error (*RMSE*)	259.25
Normalized root mean square error (*NRMSE;* %)	28.85
Akaike information criterion	145.67

https://doi.org/10.17221/191/2022-JFS

Table 4. Parameters of the regression model for sap flow estimation of tree group (model 2)

Variable	Estimate	Standard deviation	*P*-value	Lower limit	Upper limit
Intercept	1 721.57	381.9	0.0011	870.64	2 572.50
Radiation	1.15×10^{-5}	4.41×10^{-6}	0.0257	1.71×10^{-6}	2.14×10^{-5}
Humidity	–18.601798	3.890516	0.0007	–27.27	–9.93

Table 5. Statistical evaluation of the regression model for sap flow estimation of tree group (model 2)

Statistical measure	Value
Coefficient of determination (R^2)	0.90
Root mean square error (*RMSE*)	143.46
Normalized root mean square error (*NRMSE;* %)	15.96
Akaike information criterion	134.20

DISCUSSION

The results demonstrated that it is possible to model sap flow based on radiation. Nevertheless, the construction of the model is somewhat difficult. Although the dependence between sap flow and incident solar radiation during the day has been demonstrated, the calculation of total daily radiation is more complex and dependent on multiple factors. In addition to radiation, other variables explaining sap flow variability are also canopy parameters such as canopy volume, canopy surface, and canopy area. Another external variable is also air humidity. When creating a regression model that differentiates individual trees, the crown parameters cannot be entered into the linear regression model because they repeat across time and the air humidity parameter repeats within the plot. Thus, these parameters do not meet the criteria for linear regression. Therefore, a Random Forest machine learning model was created, which allows adding variables that do not meet the normal distribution criterion and allows adding autocorrelated variables. At the same time, it is evident that other factors could explain the residual variability, especially the health status of the trees.

A high correlation between sap flow and global radiation is known from previous studies. In the study by Bužková et al. (2015), the correlation coefficient between the sap flow of individual trees and incident global radiation reached values from $r = 0.82$ up to $r = 0.97$ during the moist condition and values from $r = 0.49$ up to $r = 0.61$ during dry conditions. Cumulative changes of diameter at breast height (*DBH*), cumulative and non-cumulative changes in volume, volumetric soil water content, stem temperature, and air temperature are also correlated with global radiation. Generally, sap flow during dry conditions has lower dynamics compared to moist days. The authors also showed an inconsistent correlation between CO_2 efflux and sap flow indicating the complexity of effects. Pokorný and Šalanská (2001) pointed out that low soil water content limited stand transpiration, particularly under high radiation conditions. Oogathoo et al. (2020) found a high dependence within the diurnal pattern of sap flow and radiation on the example of balsam fir and black spruce, but also found a significant dependence between sap flow and vapour pressure deficit. The response of sap flow to global radiation and *VPD* on a daily basis generally exhibits a hysteresis phenomenon. Such hysteresis can be linked with the existence of a time lag between two-time series when one lags the other for a certain time, resulting in an asynchronous rise and fall of the two variables on a daily basis (Zhang et al. 2014).

In this study, the sum of global radiation and the sum of sap flow for the whole day was used. This is due to the existence of a time lag in the sap flux response to incoming short-wave solar radiation. Wan et al. (2023) evaluated the time lags of sap flux with the incoming short-wave solar radiation and vapor pressure deficit for 52 tree species. The time lag between solar radiation and sap flow varies from 0.16 to 2.81 h in different species with an average of 1.34 h (*SD* ± 0.62 h), while the time lag between sap flow and VPD varies from –1.14 to 2.24 h with an average of 0.67 h (*SD* ± 0.86 h). The time lag is controlled by meteorological properties, soil

https://doi.org/10.17221/191/2022-JFS

moisture and tree sapwood area (Wan et al. 2023). Because we did not monitor all these parameters, it was not possible to determine the value of the time lag, or this value varied respectively. Therefore, we did not model the daily sap flow, but worked with the sum of solar radiation and sap flow for selected days.

The values of the correlation coefficients between sap flow and global radiation in the above studies are broadly consistent with the regression rebate of our linear regression model for sap flow estimation using the radiation model applied to the canopy height model (the coefficient of determination R^2 = 0.66 corresponds to a correlation coefficient value of r = 0.81). The output quality of prediction algorithms highly depends on how well the input variables represent the ecosystem and the target variables (Pan et al. 2020). Ellsäßer et al. (2020) confirmed that canopy area, as well as relative humidity, have the greatest impact when predicting sap flow too.

However, most of the published studies are based on direct measurements of radiation using sensors. This approach is preferable if we want to capture the pattern of changes in radiation due to weather changes (especially cloud cover). In contrast, the calculation procedure used allows the calculation of radiation incidents on individual tree crowns and thus includes the effect of mutual shading of the tree crowns. The solar radiation calculation tool contains two important parameters that strongly influence the value of the calculated radiation: transmittance and diffuse proportion. Transmittivity is a property of the atmosphere that is expressed as the ratio of the energy reaching the Earth's surface to that which is received at the upper limit of the atmosphere. The diffuse proportion is the fraction of global normal radiation flux that is diffuse (ESRI 2020). If a model were built with global radiation measured by a sensor, the model would probably reach a higher quality. The actual measured radiation may be different from the theoretically calculated one due to single cloud overflight etc.

CONCLUSION

Based on sap flow measurements on selected trees in the test area with subsequent UAV imaging, the relationship between the total daily sap flow and the incident global radiation calculated in a GIS environment based on the created DSM was established. The developed model allows to calculate the total daily sap flow also for the whole stand by calculating the basic parameters of individual trees such as canopy area, canopy surface and total daily global radiation. However, it is not possible to apply the results to a larger area, as the model developed is likely to be only locally effective. Further analyses at multiple sites in forest stands with different species, age and spatial structure are needed for a universal application of such models. Future studies will need to focus on the development of a model describing daily sap flow in hour intervals. This will require analysing the influence of other factors such as soil water content, tree health and various meteorological conditions. Different techniques such as Fourier transform or convolutional and recurrent neural networks would be used to create such time series models.

The area transpiration map can be created not only from the UAV data but also, for example, using airborne laser scanning data, since if the results are sufficiently verified, it will be possible to calculate transpiration based on the identification of individual trees from the digital surface model and their crowns and the subsequent calculation of global radiation. Nevertheless, this will always be quite generalised data. However, the estimation procedure developed can be used at least in a framework for hydrological analyses to determine the influence of vegetation on the water cycle in the landscape. By using a drone or airborne laser scanning data for model building, it is possible to estimate forest cover transpiration at the individual tree level.

Acknowledgement: We thank the Czech Forest Management Institute and Czechglobe – Global Change Research Institute of the Czech Academy of Sciences for the data provided for the purpose of this study.

REFERENCES

Allen R.G, Pereira L.S, Raes D., Smith M. (1998): Crop Evapotranspiration: Guidelines for Computing Crop Water Requirements. FAO Irrigation and Drainage Paper 56. Rome, FAO: 300.

Baker J.M., van Bavel C.H.M. (1987): Measurement of mass flow of water in the stems of herbaceous plants. Plant, Cell & Environment, 10: 777–782.

https://doi.org/10.17221/191/2022-JFS

Barrett D.J., Hatton T.J., Ash J.E., Ball C.M. (1996): Transpiration by trees from contrasting forest types. Australian Journal of Botany, 44: 249–263.

Bond B.J., Jones J.A, Moore G., Phillips N., Post D., McDonnell J.J. (2002): The zone of vegetation influence on baseflow revealed by diel patterns of streamflow and vegetation water use in a headwater basin. Hydrological Processes, 16: 1671–1677.

Brenner C., Thiem C.E., Wizemann H.D., Bernhardt M., Schulz K. (2017): Estimating spatially distributed turbulent heat fluxes from high-resolution thermal imagery acquired with a UAV system. International Journal of Remote Sensing, 38: 3003–3026.

Bužková R., Acosta M., Dařenová E., Pokorný R., Pavelka M. (2015): Environmental factors influencing the relationship between stem CO_2 efflux and sap flow. Trees, 29: 333–343.

Caspari H.W., Green S.R., Edwards W.R.N. (1993): Transpiration of well-watered and water-stressed Asian pear trees as determined by lysimetry, heat-pulse and estimated by a Penman-Monteith model. Agricultural and Forest Meteorology, 67: 13–27.

Choi Y., Suh J., Kim S.M. (2019): GIS-based solar radiation mapping, site evaluation, and potential assessment: A review. Applied Sciences, 9: 1960.

Čermák J., Deml M. (1974): Method of water transport measurements in woody species, especially in adult trees (in Czech). Patent (Certification of authorship) CSFR, 155622: 5997–1972.

Čermák J., Kučera J., Nadezhdina N. (2004): Sap flow measurements with some thermodynamic methods, flow integration within trees and scaling up from sample trees to entire forest stands. Trees, 18: 529–546.

Dou X., Yang Y. (2018): Evapotranspiration estimation using four different machine learning approaches in different terrestrial ecosystems. Computers and Electronics in Agriculture, 148: 95–106.

Ellsäßer F., Stiegler C., Röll A., June T., Knohl A.; Hölscher D. (2020): Predicting evapotranspiration from drone-based thermography – A method comparison in a tropical oil palm plantation. Biogeosciences, 18: 861–872.

EMS (2018): Sap flow system EMS 81. User's manual – 2nd issue. Available at: http://www.emsbrno.cz/p.axd/en/Sap.flow.system.EMS81.SDI_t_12.html (accessed Dec 22, 2022)

ESRI (2020): An overview of the Solar Radiation toolset. Available at: https://pro.arcgis.com/en/pro-app/latest/tool-reference/spatial-analyst/an-overview-of-the-solar-radiation-tools.htm (accessed Dec 19, 2020).

Feng Y., Cui N., Gong D., Zhang Q., Zhao L. (2017): Evaluation of random forests and generalized regression neural networks for daily reference evapotranspiration modelling. Agricultural Water Management, 193: 163–173.

Fu P. (2000): A geometric solar radiation model with applications in landscape ecology. [Ph.D. Thesis.] Lawrence, University of Kansas.

Granier A. (1985): A new method of sap flow measurement in tree stems. Annales des Sciences Forestières, 42: 193–200.

Gribovszki Z., Kalicz P., Szilágyi J., Kucsara M. (2008): Riparian zone evapotranspiration from diurnal groundwater level fluctuations. Journal of Hydrology, 349: 6–17.

Hofierka J., Šúri M. (2002): The solar radiation model for Open source GIS: Implementation and applications. In: Proceedings of the Open Source GIS – GRASS Users Conference 2002, Trento, Sept 11–13, 2002: 51–70.

Huber B. (1932): Beobachtung und Messung pflanzlicher Saftströme. Berichte der Botanischen Gesellschaft, 50: 89–109. (in German)

Janata P., Klimánek M., Lukas V., Machala M., Mikita T., Nedorost J., Ždímal V. (2016): Využití dálkově pilotovaných leteckých systémů v zemědělství, lesnictví a krajinné ekologii. 1st Ed. Brno, Mendelova univerzita v Brně: 130. (in Czech)

Kučera J., Čermák J., Penka M. (1977): Improved thermal method of continual recording the transpiration flow rate dynamics. Biologia Plantarum, 19: 413–420.

Kupec P., Deutscher J. (2017): Influence of stand transpiration on diurnal streamflow in the recipient in an upland forested microwatershed during precipitation-free periods. Zprávy lesnického výzkumu, 62: 234–241. (in Czech)

Loustau D., Berbigier P., Roumagnac P., Arruda-Pacheco C., David J.S., Ferreira M.I., Pereira J.S., Tavares R. (1996): Transpiration of a 64-year-old maritime pine stand in Portugal. Oecologia, 107: 33–42.

Martin T.A. (1999): Winter season tree sap flow and stand transpiration in an intensively-managed loblolly and slash pine plantation. Journal of Sustainable Forestry, 10: 155–163.

Mikita T., Klimánek M., Cibulka M. (2013): Evaluation of airborne laser scanning data for tree parameters and terrain modelling in forest environment. Acta Universitatis Agriculturae et Silviculturae Mendelianae Brunensis, 61: 1339–1347.

Nadezhdina N., Čermák J., Nadezhdin V. (1998): Heat field deformation method for sap flow measurements. In: Proceedings of 4th International Workshop on Measuring Sap Flow in Intact Plants, Židlochovice, Oct 3–5, 1998: 72–92.

Niu H., Hollenbeck D., Zhao T., Wang D., Chen Y. (2020): Evapotranspiration estimation with small UAVs in precision agriculture. Sensors, 20: 6427.

Oogathoo S., Houle D., Duchesne L., Kneeshaw D. (2020): Vapour pressure deficit and solar radiation are the major drivers of transpiration of balsam fir and black spruce tree species in humid boreal regions, even during a short-term drought. Agricultural and Forest Meteorology, 291: 108063.

https://doi.org/10.17221/191/2022-JFS

Pan S., Pan N., Tian H., Friedlingstein P., Sitch S., Shi H., Arora V.K., Haverd V., Jain A.K., Kato E., Lienert S., Lombardozzi D., Nabel J.E.M.S., Ottlé C., Poulter B., Zaehle S., Running S.W. (2020): Evaluation of global terrestrial evapotranspiration by state-of-the-art approaches in remote sensing, machine learning, and land surface models. Hydrology and Earth System Sciences, 24: 1485–1509.

Pokorný R., Šalanská P. (2001): Sap flux of dominant trees under low soil water availability. Beskydy, 14: 99–106.

Rich P.M., Dubayah R., Hetrick W.A., Saving S.C. (1994): Using viewshed models to calculate intercepted solar radiation: Applications in ecology. American Society for Photogrammetry and Remote Sensing Technical Papers: 524–529.

Rich P.M., Fu. P. (2000): Topoclimatic habitat models. In: Proceedings of the 4th International Conference on Integrating GIS and Environmental Modeling, Banff, Sept 2–8, 2000: 14.

Sakuratani T. (1981): A heat balance method for measuring water flux in the stem of intact plants. Journal of Agricultural Meteorology, 37: 9–17.

Schiller G., Cohen Y. (1995): Water regime of a pine forest under a Mediterranean climate. Agricultural and Forest Meteorology, 74: 181–193.

Shan J., Toth C.K. (2017): Topographic Laser Ranging and Scanning. 2nd Ed. Boca Raton, CRC Press: 654.

Vincent L., Soille P. (1991): Watersheds in digital spaces: An efficient algorithm based on immersion simulations. IEEE Transactions on Pattern Analysis and Machine Intelligence, 13: 583–598.

Wan L., Zhang Q., Cheng L., Liu Y, Qin S., Xu J., Wang Y. (2023): What determines the time lags of sap flux with solar radiation and vapor pressure deficit? Agricultural and Forest Meteorology, 333: 109414.

Wondzell S.M., Gooseff M.N., McGlynn B.L. (2009): An analysis of alternative conceptual models relating hyporheic exchange flow to diel fluctuations in discharge during baseflow recession. Hydrological Processes, 24: 686–694.

Wullschleger S.D., Meinzer F.C., Vertessy R.A. (1998): A review of whole-plant water use studies in tree. Tree Physiology, 18: 499–512.

Xu J., Ma L. (2007): Relationship between effective solar radiation and sap flow process during an entire growing season in Western Mountains of Beijing. Forestry Studies in China, 9: 251–255.

Zhang Q., Manzoni S., Katul G., Porporato A., Yang D. (2014): The hysteretic evapotranspiration-vapor pressure deficit relation. Journal of Geophysical Research, 119: 125–140.

Received: December 22, 2022
Accepted: June 19, 2023